Desalination and Water Treatment
www.deswater.com

doi: 10.5004/dwt.2017.21306

85 (2017) 298–312
August

Adsorption of Cr(VI) ions from aqueous systems using thermally sodium organo-bentonite biopolymer composite (TSOBC): response surface methodology, isotherm, kinetic and thermodynamic studies

Mohammad Hadi Dehghani[a,b,c,*], Ahmad Zarei[d,*], Alireza Mesdaghinia[b], Ramin Nabizadeh[b], Mahmood Alimohammadi[b], Mojtaba Afsharnia[d]

[a]*Institute for Environmental research, Center for Water Quality Research, Tehran University of Medical Sciences, Tehran, Islamic Republic of Iran, Tel. +98 21 42933227; Fax: +98 21 66419984; email: hdehghani@tums.ac.ir*
[b]*Department of Environmental Health Engineering, School of Public Health, Tehran University of Medical Sciences, Tehran, Islamic Republic of Iran, emails: mesdaghinia@sina.tums.ac.ir (A. Mesdaghinia), rnabizadeh@tums.ac.ir (R. Nabizadeh), m_alimohammadi@tums.ac.ir (M. Alimohammadi)*
[c]*Institute for Environmental Research, Center for Solid Waste Research, Tehran University of Medical Sciences, Tehran, Islamic Republic of Iran*
[d]*Department of Environmental Health Engineering, School of Public Health, Gonabad University of Medical Sciences, Gonabad, Islamic Republic of Iran, Tel. +98 5157223514; emails: a.zarei.tums@gmail.com (A. Zarei), mafsharnia2000@yahoo.com (M. Afsharnia)*

Received 22 March 2017; Accepted 4 August 2017

ABSTRACT

Chromium, as a serious environmental contaminant, is frequently encountered in different industrial effluents. In the present study, we focused on the combined application of a surfactant-modified bentonite and chitosan for the removal of Cr(VI). In addition, the effects of several important parameters such as pH (2–8), adsorbent dosage (0.1–1.5 g/L), Cr(VI) concentration (20–200 mg/L) and contact time (60–240 min) were also investigated and the process was optimized by means of response surface methodology. The analysis of variance of the quadratic model demonstrates that the model was highly significant. Optimized values of pH, adsorbent dosage, initial Cr(VI) concentration and contact time were found to be 3.7, 1.40 g/L, 77 mg/L and 180 min, respectively. The results revealed that the prepared adsorbent had significant adsorption capacity (124.1 mg/g) for Cr(VI). All results showed that thermally sodium organo-bentonite biopolymer composite (TSOBC) had a good affinity toward Cr(VI). Among the isotherm models tested, Langmuir isotherm model was found to be the best fit for the obtained data. The adsorption kinetics indicated that Cr(VI) adsorption on TSOBC followed pseudo-second-order better than pseudo-first-order model. Moreover, thermodynamic studies showed that adsorption of Cr(VI) on TSOBC was spontaneous and endothermic in nature. The applied adsorbent was characterized by scanning electron microscopy, X-ray diffraction, energy dispersive X-ray and Fourier-transform infrared spectroscopic techniques.

Keywords: Adsorption; Cr(VI); Modified bentonite; Chitosan

---

* Corresponding author.

1. Introduction

Nowadays, contamination of various water resources by heavy metals is of great concern due to their toxicological effects on humans, animals and biota present in the environment [1–3]. Chromium, one of these metals is a serious environmental contaminant, which is frequently encountered in different industrial effluents, for example, from mining, leather tanning, electroplating and processing, manufacture of automobile parts, textile, dyeing, petroleum and fertilizer industries, etc. [4]. In the environment, chromium exists in two major states as trivalent, that is in the cationic form as Cr(III), and hexavalent Cr(VI) as anions: $HCrO_4^-$, CrO_4^{2-} and $Cr_2O_7^{2-}$ [5,6]. The cationic form is relatively immobile and innocuous [7], whereas Cr(VI) is carcinogenic and mutagenic and it is considered as one of the most harmful materials to human health by the EPA [8]. It has a high solubility and mobility in soil and aquatic systems. Therefore, it is very essential to treat Cr(VI) containing effluents before their discharge into the environment in order to prevent the deleterious impact of Cr(VI) on the environment and human health. Many techniques have been developed over the years for the removal of toxic metals from water and wastewater including chemical precipitation, bioadsorption, ion-exchange, evaporation, advanced oxidation processes, complexation, membrane separation, electrolysis, reverse osmosis, biological treatment and nanoparticles [9–22]. Recently, bioadsorption techniques using natural biopolymers including chitin and chitosan composites have been developed due to their biocompatibility, biodegradability, non-toxicity, abundance in nature, chelating ability with heavy metals and cost-effectiveness to adsorb heavy metals as an alternative to conventional wastewater treatment processes, even at low concentrations [23]. Commonly, chitosan results from the deacetylation of chitin with a strong alkaline solution [24], which is abundantly available in nature as a major component of crustacean shells such as insects, crabs, prawns and shrimps [25].

Chitosan is an excellent adsorbent for the removal of many contaminants including almost all the metal ions and dyes from aqueous solution due to the presence of amine ($–NH_2$) and hydroxyl (–OH) groups in its structure [26]. Moreover, chitosan is a cationic polymer and has the ability to adsorb many negatively charged ions from aqueous environment [27]. From the other side, chitosan easily degrades and becomes soluble in acidic media, which might be a limiting step for its applicability. Therefore, chitosan can be cross-linked to render it insoluble in acidic environment. Furthermore, to improve its adsorption capacity and resistance to acidic environment, chitosan can be coated on other materials to form biocomposites [28]. In literature, various types of solid materials have been coated with chitosan such as perlite [29], bentonite [30], montmorillonite, activated clay [31–33], alumina [34], silica and calcium alginate as support [35]. In the present study, the adsorption capability of chitosan was improved by the incorporation of modified bentonite.

Bentonite, as a widely distributed, abundant and low-cost mineral worldwide, is effective for immobilizing toxic contaminants and has high adsorptive and ion-exchange properties [36]. However, raw bentonite cannot effectively adsorb Cr(VI) anionic states from aqueous environment due to negative charge on its surface. Therefore, it can often be modified using a variety of physical and chemical methods to achieve the desired surface properties [37]. Several researchers have used cationic quaternary amine compounds or surfactants for the modification of clay minerals as organoclays. Organoclays have high sorption potential toward various hydrophobic organic contaminants [38] and heavy metals [39,40]. In fact, modifications of bentonite with cationic surfactants have attracted considerable attention because they provide bentonite with the potential to behave as anionic exchangers and change its surface properties from hydrophilic to hydrophobic [41,42]. Moreover, the space of the layers also greatly increases. Bentonite is superior compared with abovementioned solid supports, because it can be easily treated by intercalating different functional groups into the montmorillonite interlayers.

In this work, bentonite was treated through three procedures: Na_2CO_3 treatment (BNa), thermal treatment and compound treatment by cetyltrimethylammonium bromide (CTAB). Na_2CO_3 enhances the rate of water adsorption and the expansion ratio of raw bentonite. Thermal treatment eliminates water from the surface or between the layers, and increases the specific surface area of the bentonite. Compound modification by a surfactant could make its water treatment influence stronger [43]. In this study, we used oxalic acid for cross-linking chitosan. It is hypothesized that the combination of chitosan with modified bentonite may create a more efficient adsorbent due to the ability of more active sites of chitosan after coating, thus, enhancing the adsorption capacity. However, to the best of our knowledge, the present methodology had not yet been reported for the removal of Cr(VI). Thus, in this study, we focused on the investigation of the application of naturally abundant and less expensive substances such as chitosan and bentonite/chitosan biocomposite in the removal of Cr(VI). In the present study, the experimental design and analysis of process parameters affecting Cr(VI) removal was done by response surface methodology (RSM) under "R" software [44].

2. Materials and methods

2.1. Reagents and apparatus

All the reagents and chemicals used in the present study were of analytical grade and without further purification. CTAB, chitosan with 90% degree of deacetylation and Ca-bentonite powder were purchased from Sigma-Aldrich (Germany). Residual concentration of Cr(VI) was determined from the absorbance of the solution measured by diphenylcarbazide method using a spectrophotometer (Unico UV-2100) at a wavelength of 540 nm. Sodium carbonate, potassium dichromate, oxalic acid, hydrochloric acid and sodium hydroxide were also purchased from Sigma-Aldrich. All pH values were determined using a Sartorius PB-11 pH meter, Germany. Double distilled water was applied for the experiments. Other instruments were shaker incubator (model Skir-601), furnace (model AK1200) and oven (Memmert, Italy). The cation exchange capacity and real density of calcium bentonite was 132.31 meq/100 g and 2.5212 ± 0.0031 g/cm^3, respectively. The chemical components of calcium bentonite as wt% were in the following order: SiO_2

(61.1), Al_2O_3 (18.43), MgO (3.33), Fe_2O_3 (3.1), Na_2O (1.8) and CaO (0.09).

2.2. Preparation of modified bentonite

In the beginning, calcium bentonite was modified through three procedures: sodium carbonate (BNa) modification, thermal and compound modification by CTAB. Initially, for sodium carbonate treatment, 500 g of the raw bentonite was added into a beaker containing ethanol solution (volume ratio = 1:1). After that, sodium carbonate in an amount equivalent to 4% of the raw bentonite was added into the solution. Then, the pH value of the suspension was adjusted to 9 by adding sodium hydroxide. The slurry was then shaken for 2 h in a shaker incubator at 80°C with frequency of 110 min^{-1}. The slurry was centrifuged at rotational frequency of 3,000 min^{-1} for 10 min. The solid residue was then washed several times with double distilled water until the absence of CO_3^{2-} was confirmed with $Ca(OH)_2$ test. The sample was then dried overnight at 105°C. For thermal treatment, the prepared sodium bentonite was transferred to a furnace for 2 h at 450°C. Finally, for compound modification, a solution of CTAB with a concentration of 20 g was prepared in a 1 L conical flask. The CTAB solution and 100 g of sodium bentonite were added to 1 L Erlenmeyer flask and agitated at 30°C for 2 h. Finally, the modified bentonite was filtered and washed several times with deionized water to remove bromide ions. The solid was then dried at room temperature during 24 h, ground in a laboratory mortar, sieved and placed in a desiccator.

2.3. Preparation of thermally sodium organo-bentonite biopolymer composite

Chitosan was coated onto bentonite according to the previous study [45]. 0.5 g chitosan 90% was slowly added into a beaker containing oxalic acid (volume fraction, 2%) solution under continuous stirring for 2 h, followed by the addition of 25 g modified bentonite. The mixture was agitated for 6 h and was later precipitated by sodium hydroxide. The preparation procedure of thermally sodium organo-bentonite biopolymer composite (TSOBC) is schematically shown in Figs. 1 and 2.

2.4. Adsorption experiments

Batch experiments, designed by RSM in "R" software, were conducted at 150 rpm and 25°C in order to explore the influence of important factors including pH (2–8), adsorbent dosage (0.1–1.5 g), initial concentrations of Cr(VI) (20–200 mg/L) and contact time (60–240 min) on the adsorption of Cr(VI) from aqueous solution by TSOBC. A stock solution (1,000 mg/L) of Cr(VI) was prepared by dissolving exact quantities of potassium dichromate ($K_2Cr_2O_7$) in deionized water. Test solutions of different concentrations were prepared by

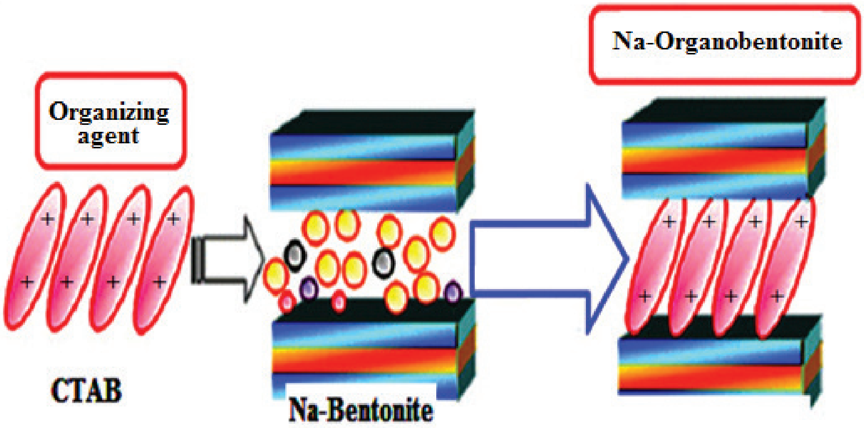

Fig. 1. Modification of thermally treated sodium bentonite by CTAB.

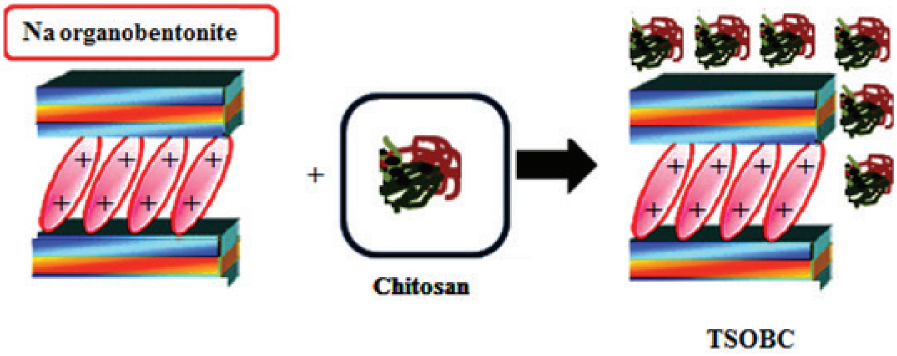

Fig. 2. Thermally sodium organo-bentonite biopolymer composite (TSOBC).

diluting the stock solution with suitable volume of distilled water. After the solution was shaken for predetermined time, it was filtered through a Whatman paper and the supernatant liquid was analyzed to find the residual Cr(VI) concentration and used to determine the removal percentage of the Cr(VI) by a spectrophotometer. The differences in concentration of Cr(VI) before and after adsorption were calculated to find out the amount of hexavalent chromium adsorbed by the adsorbent. A desired quantity of TSOBC was added to 1 L of known concentration of Cr(VI) ions and pH in a 100 mL volumetric flask and kept in an incubator shaker at fixed agitation speed (150 rpm) for various time intervals. The maximum adsorption capacity was obtained from the isotherm study. The equilibrium isotherms were fitted to the Langmuir, Freundlich and Temkin models. Kinetic and thermodynamic studies were also carried out. Experiments were conducted in duplicate and mean values were taken. The removal percentage and also the amount of Cr(VI) adsorbed at equilibrium conditions, Q_t (mg/g), were calculated by the following equations:

$$Q_t = \frac{(C_0 - C_e)V}{W} \tag{1}$$

$$\%\ \text{Removal} = \frac{(C_0 - C_e) \times 100}{C_0} \tag{2}$$

where C_0 and C_e denote the initial and equilibrium Cr(VI) concentrations (mg/L), respectively. V is the volume of the solution (L) and W is the mass of the adsorbent used (g).

2.5. Experimental design

In the present study, the standard RSM design called central composite design was used to determine the regression model equations and operating conditions for adsorption of Cr(VI) ions using TSOBC. The RSM was employed to evaluate the combined effects of pH (X_1), TSOBC dose (X_2), initial Cr(VI) concentration (X_3) and time (X_4) on the adsorption process. In the experimental design model, pH (2–8), TSOBC dose (0.1–1.5 g), initial Cr(VI) concentration (20–200 mg/L) and time (60–240 min) were taken as input variables. Percentage removal of Cr(VI) was taken as the response of the adsorption system. The chosen independent variables used in these experiments were coded by the following equation:

$$A_i = \frac{X_i - X_0}{\Delta X} \tag{3}$$

where A_i is the dimensionless coded value of the ith independent variable, X_i is the uncoded value of the ith test variable, X_0 is the value of X_i at the center point and ΔX is the step change value.

Experimental design of independent variables and levels considered for Cr(VI) adsorption is given in Table 1. Totally, 44 experiments were designed, consisting of 2 × 4 = 8 axial points, 2^4 = 16 design points and 20 center points. The details of the designed experiments are given in Table 2. A quadratic (second-order) model as shown in Eq. (4) was applied to approximate the interaction between the response (Y) and four independent variables:

$$Y = b_0 + \Sigma_{i=1}^{k} b_i X_i + \Sigma_{i=1}^{k} b_{ii} X_i^2 + \Sigma_{i=1}^{k-1} 1 \Sigma_{i=2}^{k} b_{ij} X_i X_j + \varepsilon \tag{4}$$

where Y represents the response variable (chromium removal efficiency); b_0 is a constant value; b_i, b_{ii} and b_{ij} refer to the regression coefficient for linear, second order and interactive effects, respectively; X_i and X_j are the independent variables and ε denotes the error of the model [46]. The fitness of regression model was evaluated by calculating coefficient of determination (R^2). Experimental design of variables and levels considered for Cr(VI) adsorption are summarized in Table 1. The tests design and also statistical analysis of the obtained data were done by use of "R" software.

Table 1
Experimental design of variables and levels considered for Cr(VI) adsorption in RSM using "R"

Factors	Symbol	Range and levels (coded)		
		–1	0	1
pH	X_1	2	5	8
TSOBC dose (g/L)	X_2	0.1	0.8	1.5
Cr(VI) concentration (mg/L)	X_3	20	110	200
Time (min)	X_4	60	150	240

3. Results and discussion

3.1. Characterization of thermally sodium organo-bentonite biopolymer composite

3.1.1. SEM analysis

Scanning electron microscopic (SEM) analysis was applied in order to confirm the adsorption of Cr(VI) on TSOBC, and to get more information regarding change of the adsorbent surface morphology after the modification. The mean particle size of TSOBC was <10 μm. Also, Brunauer–Emmett–Teller surface area of fabricated particles was 80 m^2/g. The SEM images are depicted in Fig. 3. As shown in the figure, the surface morphology of the TSOBC appears to change significantly following after Cr(VI) adsorption. It can be observed that the surface of the TSOBC was rough with crispy appearance. It can be clearly seen that TSOBC, after Cr(VI) adsorption loses its coarse structure and gain more smooth surface, confirming that the adsorption of chromium has occurred. The image of the adsorbent also presents blocking of pores due to the adsorption of chromium in the porous parts of TSOBC. In the other words, the decrease of porosity on the TSOBC surface might be due to the adsorption of precipitated chromium ions and their placement on the surface and also inside the pores. SEM images of TSOBC before and after Cr(VI) adsorption were obtained using a VEGA/TESCAN SEM. The surface morphology of TSOBC before adsorption was different from that of after adsorption.

3.1.2. XRD and EDX analyses

X-ray diffraction (XRD) patterns of different samples including sodium bentonite (BNa), BNa-CTAB, chitosan, chitosan–oxalic acid and TSOBC are presented in Fig. 4.

Table 2
Experimental design for Cr(VI) removal by TSOBC

Run order	X_1	X_2	X_3	X_4	Efficiency %	Run order	X_1	X_2	X_3	X_4	Efficiency %
1	5	0.8	110	150	65	23	6.5	1.15	155	105	27.1
2	5	0.8	110	150	64.6	24	5	0.8	110	150	63.9
3	3.5	0.45	155	195	45.7	25	3.5	1.15	155	195	86.5
4	3.5	1.15	65	105	73.9	26	5	0.8	110	150	62.4
5	6.5	1.15	65	195	72	27	3.5	1.15	65	195	96.7
6	6.5	1.15	65	105	56	28	3.5	0.45	65	105	44.9
7	5	0.8	110	150	59.6	29	8	0.8	110	150	20
8	6.5	0.45	155	105	12.5	30	5	0.8	110	150	64.7
9	5	0.8	110	150	64.1	31	5	0.8	110	150	58.1
10	5	0.8	110	150	59.9	32	5	0.8	110	150	59.3
11	3.5	0.45	65	195	49.4	33	5	0.8	110	150	63.8
12	6.5	0.45	65	195	31	34	5	0.8	110	150	63.9
13	5	0.8	110	150	64.9	35	2	0.8	110	150	59.5
14	3.5	0.45	155	105	34.9	36	5	0.8	200	150	54.9
15	5	0.8	110	150	64.5	37	5	0.8	20	150	76.9
16	5	0.8	110	150	62.8	38	5	0.1	110	150	15.8
17	5	0.8	110	150	60.9	39	5	0.8	110	150	69.3
18	3.5	1.15	155	105	52	40	5	0.8	110	240	64.4
19	6.5	1.15	155	195	58.8	41	5	1.5	110	150	74.8
20	6.5	0.45	155	195	33.6	42	5	0.8	110	60	24.3
21	5	0.8	155	150	62.5	43	5	0.8	110	150	61.5
22	6.5	0.45	65	105	28.7	44	5	0.8	110	150	62.1

Fig. 3. SEM micrograph of TSOBC: before (a) and after (b) Cr(VI) adsorption, schematic of fabricated TSOBC (c).

A typical diffraction band of BNa is 5.75°, corresponding to a basal spacing of 1.23 nm. After intercalation with surfactant, the typical diffraction peak of bentonite moves to lower angle (4.412°), corresponding to a basal spacing of 1.95 nm. The predominant peaks belong to the quartz (Q) and montmorillonite (M). Chemical and thermal modification changed the bentonite structure, reducing the intensity of the typical peak of montmorillonite, inducing a possible displacement in octahedral and tetrahedral layers arrangement. The X-ray diffraction analysis of TSOBC showed an increase in d-spacing compared with BNa, confirming the formation of intercalated structures. The adsorption of Cr(VI) on the surface of TSOBC was also confirmed from the energy dispersive X-ray (EDX) spectrum (Fig. 5) which shows the presence of chromium with the other elemental constituents.

3.1.3. FTIR analysis

Fig. 6 shows the Fourier transform infrared (FTIR) spectra of CTAB, oxalic acid, chitosan, sodium bentonite, CTAB bentonite and TSOBC. The typical absorption band of chitosan (Fig. 6(c)) at 1,593 cm^{-1} belongs to the characteristic peak of $-NH_2$, confirming that the used chitosan have high degree of deacetylation [47]. While the TSOBC (Fig. 6(f)) exhibits a disappearance of the band at 1,593 cm^{-1}, indicating the formation of a new band at 1,666 cm^{-1} which are related to the consumption of $-NH_2$. Furthermore, the absorption band at 3,443 cm^{-1} was assigned to hydroxyl group. The band at 1,019 cm^{-1} in sodium bentonite (Fig. 6(d)) was related to Si–O stretching vibrations. Compared with sodium bentonite, the characteristic absorption bands of the bending vibrations of $-CH_3$ (1,469 cm^{-1}), the asymmetric and symmetric stretching vibrations of $-CH_3$ (2,921 cm^{-1}) and $-CH_2$ (2,849 cm^{-1}) were observed on the FTIR spectra of bentonite modified with CTAB. This means that the CTAB molecule was intercalated

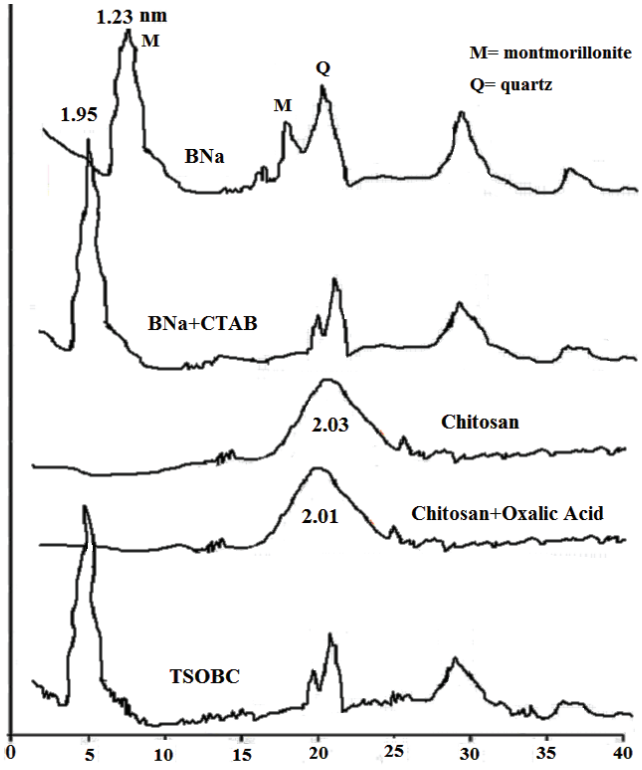

Fig. 4. XRD patterns of the samples.

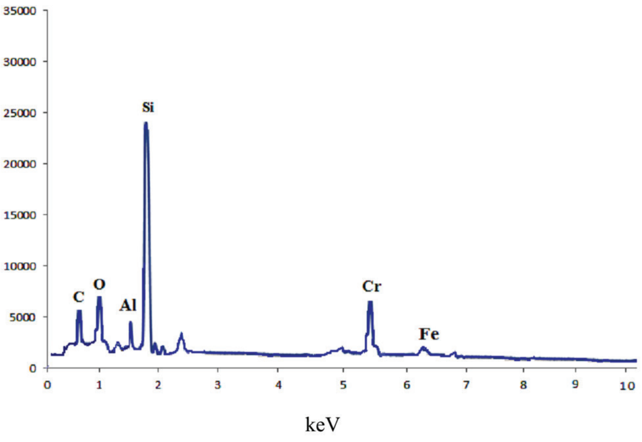

Fig. 5. Energy dispersive X-ray (EDX) spectrum of the adsorbed Cr(VI) by TSOBC.

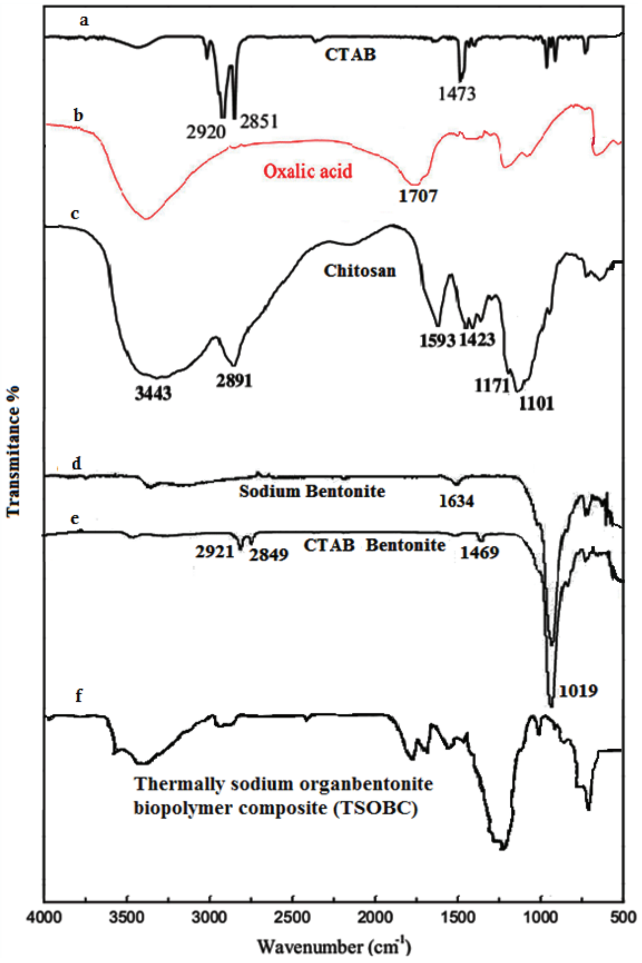

Fig. 6. FTIR spectra of (a) CTAB, (b) oxalic acid, (c) chitosan, (d) sodium bentonite, (e) CTAB bentonite and (f) TSOBC.

into the interlayer space of sodium bentonite. The absorption peak at 1,634 cm^{-1} (Fig. 6(d)) belongs to –OH bending vibration of H_2O molecule in sodium bentonite structure. It is noteworthy that the intensity of this absorption peak of CTAB bentonite reduces, which confirms the H_2O content reduced due to the replacement of the hydrated cations by cations of the surfactant. After modification of sodium bentonite by CTAB, the surface properties of bentonite changed from hydrophilic to hydrophobic [48].

3.2. Fitting the process model

The removal efficiency of Cr(VI) depends on the individual and combinations of experimental variables and the results show a significant variation for each combination. Empirical relationships between the response and the independent variables have been expressed by the following quadratic model:

$$\begin{aligned}\text{Efficiency}_{\text{Cr(VI)}} = {} & 63.07 - 20.27X_1 + 30.02X_2 - 11.77X_3 \\ & + 18.65X_4 - 6.52X_1X_2 - 11.72X_2X_3 + 16.57X_2X_4 \\ & + 13.12X_3X_4 - 22.47\,X_1^2 - 16.92\,X_2^2 + 4.20\,X_3^2 \\ & - 17.87\,X_4^2 \end{aligned} \quad (5)$$

where X_1, X_2, X_3 and X_4 are solution pH, the adsorbent dosage, initial Cr(VI) concentration and contact time, respectively.

The values of negative coefficients indicate that individual or double interactions items negatively affect Cr(VI) removal (i.e., adsorption removal percentage decreases), whereas positive coefficients mean that items increase Cr(VI) adsorption in the studied range. In this case, X_1, X_2, X_3, X_4, X_1X_2, X_2X_3, X_2X_4, X_3X_4, X_1^2, X_2^2, X_3^2 and X_4^2 are significant model terms (Table 3). Analysis of variance (ANOVA) has been used to analyze the accessibility of the model. The results of ANOVA for the response are summarized in Table 4. The quality of the fitted model was described by the coefficient of determination R^2. The R^2 value gives the proportion of the total variation in the response predicted by the model and a higher R^2 value (close to 1) is more desirable. In these experiments, the values of multiple R^2 and adjusted R^2 for Cr(VI) adsorption were, 0.984 and 0.976, respectively, showing a satisfactory adjustment for the reduced quadratic model to the experimental data. This result means that 97.6% of the total variation on Cr(VI) removal data can be described by the selected model. The larger the value of T and the smaller the value of P, the more significant is the corresponding parameter in the regression model. Corresponding values of T and P were 102.47 and 0.000 which suggest the significance of the constant for regression coefficient. The significance and quality of each coefficient was also described by F and P values. The higher F value (362.72) and accordingly lower P value (0.000) in Table 4 implies that the second-order polynomial model is statistically significant, in other words, the model fitted well with the experimental results [11,49]. The lack of fit (LOF) test evaluates the goodness of fit and must be insignificant in a well fitted model [50]. The LOF value for the experiments was 0.3698 (Table 4). Fig. 7 shows the normal probability plot of residuals for Cr(VI) adsorption efficiency. Results of ANOVA for Cr(VI) removal are shown in Table 4.

Table 3
Estimated parameters and their significance

Variable	Coefficient estimate	Standard error	*T* Value	*P* Value
Intercepts	63.07	0.61	102.47	2.2e–16
X_1	–20.27	1.11	–18.25	2.2e–16
X_2	30.02	1.11	27.03	2.2e–16
X_3	–11.77	1.08	–10.80	1.1e–11
X_4	18.65	1.11	16.80	2.65e–07
X_1X_2	–6.52	2.72	–2.39	0.023
X_2X_3	–11.72	2.72	–4.31	0.0001
X_2X_4	16.57	2.72	6.09	1.2e–06
X_3X_4	13.12	2.72	4.82	4.1e–05
X_1^2	–22.47	1.85	–12.10	7.3e–13
X_2^2	–16.92	1.85	–9.11	5.1e–10
X_3^2	4.20	1.85	2.26	0.03
X_4^2	–17.87	1.85	–9.62	1.5e–10

3.3. Effect of process variables

3.3.1. Effect of pH and adsorbent dosage

The pH of the solution is an important parameter that determines the amount of contaminant adsorbed [51]. The effect of solution pH on Cr(VI) removal by TSOBC was investigated in the pH range of 2–8. The combined effect of initial pH and adsorbent dosage on adsorption efficiecny can be predicted from the plots shown in Fig. 8. At the highest level of studied pH 8, the percentage removal was low, 20%. The percentage removal of Cr(VI) by TSOBC was studied in specified range of pH 2–8. Cr(VI) removal showed to be very

Table 4
Analysis of variance (ANOVA) of the response surface quadratic model for Cr(VI) adsorption

Sources	Degrees of freedom	Sum of squares	Mean square	*F* Value	Prob > *F*
Second-order response	4	10,734.8	2,683.70	362.72	2.2e–16
Pure quadratic response	4	2,784.5	696.14	94.08	3.5e–16
Residuals	29	214.6	7.40	–	–
Lack of fit	11	89.5	8.14	1.17	0.3698
Pure error	18	125.1	6.95	–	–

Note: *F* Statistic: 136.6 on 14 and 29 DF, *P* value: <2.2e–16, multiple R^2: 0.984, adjusted R^2: 0.976, lack of fit: 0.3698.

sensitive to pH variation, both in low and high adsorbent doses. Fig. 8 obviously depicts that the sorption efficiency of TSOBC depends on the solution pH, increasing with a decrease in pH and thus maximum adsorption was occurred in the acidic conditions. Under strong acidic environment (pH < 2), chitosan undergoes dissolution and solidifies in alkaline media [52,53], which decreases the removal percentage. This correlates with the experimental data obtained at lower pH for TSOBC. Moreover, the extent of Cr(VI) adsorption on TSOBC is dependent on the stability and affinity of chromium species. In low concentration with pH in the range of 2.0–6.5, hexavalent chromium exists as hydrogen chromate anions $HCrO_4^-$, and it exists as chromate ions CrO_4^{2-} at pH > 8 [54]. The fraction of any particular species is dependent upon pH and Cr(VI) concentration. These anions have tendency to bind to the protonated amine functional groups of the chitosan. At pH 6.0, chitosan presents both reactive forms $–NH_3$ and $–NH_2$ and Cr(VI) forms $HCrO_4^-$ (~75%) and CrO_4^{2-} (~25%) at 25°C, suggesting that the behavior of Cr(VI) adsorption by chitosan occurred by chelation and electrostatic interaction with the amine groups of chitosan. At pH < 4, the amine group on chitosan, the main reason for chromium adsorption, is protonated to varying degree which in general increases the removal efficiency. Decrease in adsorption at pH > 7.0 is due to precipitation of insoluble chromium hydroxide on the available binding sites on the adsorbent surface. Another reason may be attributed to decline of protonation of chitosan surface at higher pH values. Almost similar trend was observed for all concentrations. In the present work, pH 3.7 was chosen as an optimum pH for the evaluation of adsorption characteristics of Cr(VI) on TSOBC. With increase in the adsorbent dose up to a certain limit at particular pH, percentage removal increases due to the availability of more sites for the adsorption of chromium ions.

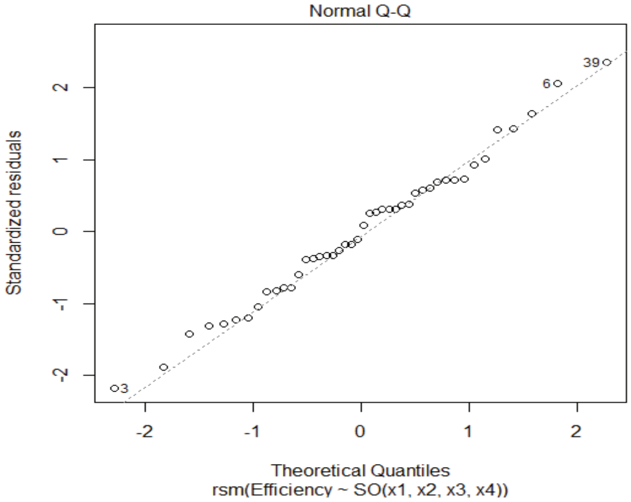

Fig. 7. Normal probability plot of residuals for Cr(VI) adsorption efficiency.

3.3.2. Effect of adsorbent dosage and contact time

The effect of TSOBC dosage was studied at the dosage between 0.1 and 1.5 g. These experiments were conducted at 25°C and 150 rpm. The effect of adsorbent dose and contact time on the removal efficiency of Cr(VI) is depicted in contour and 3D plots in Fig. 9. Though cross-linking process was at the cost of the loss of some active binding sites such as amino and hydroxyl groups, and decreased the binding sites for chromium, chitosan intercalated in bentonite by cross-linking process, and an increase in interlayer spacing was seen. The more interlayer spacing enhanced the adsorption of Cr(VI) ions onto TSOBC, leading to an increase in adsorption. In this study, it is found that the removal of Cr(VI) ions increased with increase in contact time up to certain time. Cr(VI) uptake was slow at first. Accordingly, most of the ultimate adsorption capacity occurred within the third hour of contact. More increase in contact time (after 180 min),

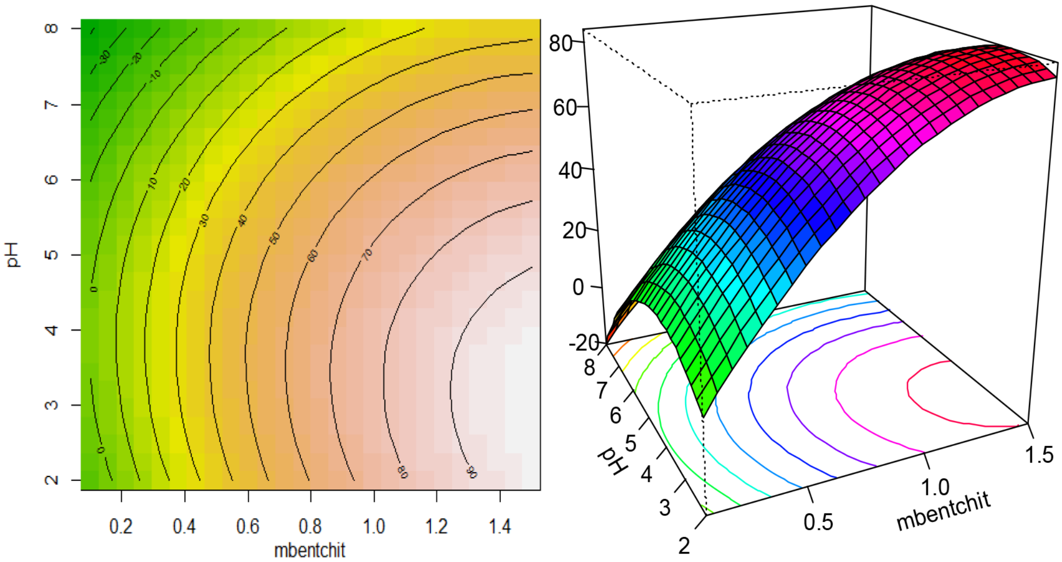

Fig. 8. Effect of pH and the adsorbent dose on the removal percentage of Cr(VI) by TSOBC.

there was a very slight increase in the uptake rate. Similarly to the contact time effect reported in the literature [55,56]. Increase in removal percentage with increase in contact time can be attributed to the fact that more time becomes available for Cr(VI) ions to make an attractive complex with TSOBC.

3.3.3. Effect of adsorbent dosage and Cr(VI) ion concentration

Fig. 10 depicts the combined effect of adsorbent dosage and Cr(VI) concentration on the percentage removal of chromium ions under predefined conditions given by "R". It is obvious that the removal efficiency of Cr(VI) ions increased with the increase in adsorbent dosage due to the availability of greater surface area and thus active adsorption sites on the adsorbent. However, once almost all Cr(VI) ions are adsorbed, the contribution of additional adsorbent dosage is insignificant. Higher adsorbent dosage and lower chromium concentration increased the chromium removal percentage.

3.3.4. Effect of Cr(VI) ion concentration and time

Different concentrations of Cr(VI) ions from 20 to 200 mg/L were tested. The combined effect of initial chromium concentration and contact time is presented in the form of counter and 3D plots (Fig. 11). It is observed that with increase

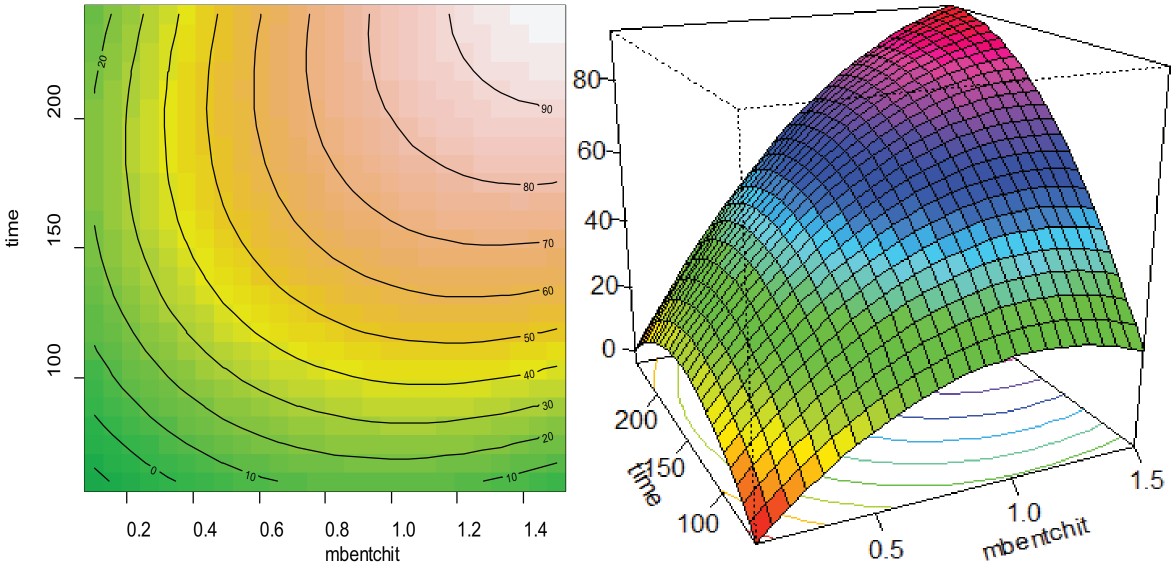

Fig. 9. Effect of adsorbent dose and contact time on the removal percentage of Cr(VI) by TSOBC.

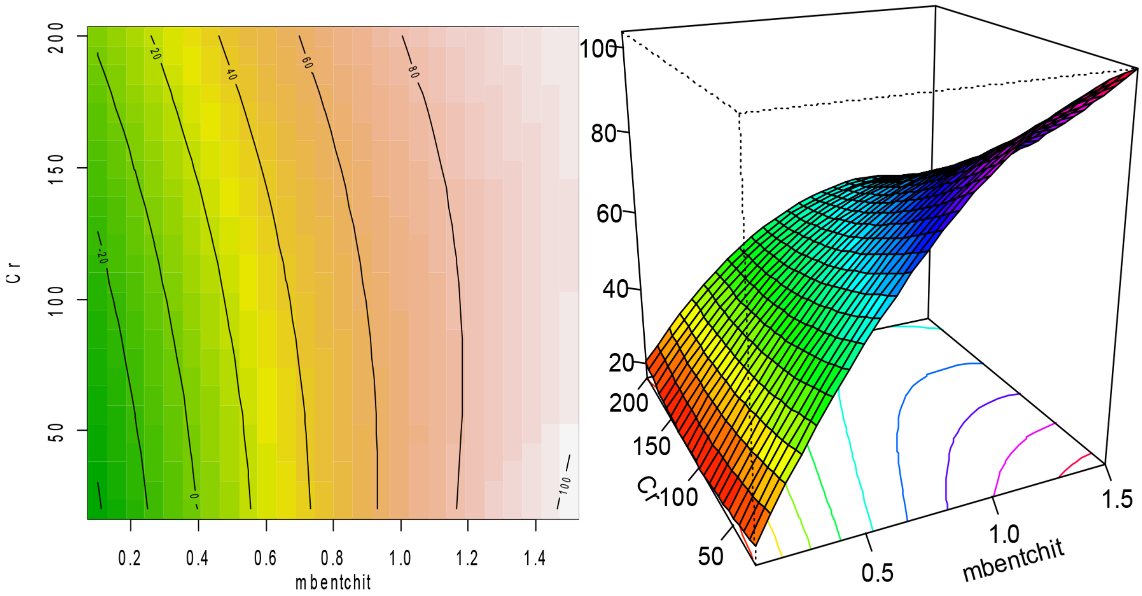

Fig. 10. Counter and 3D plots showing the effect of adsorbent dose and chromium concentration on the adsorption of Cr(VI) ions by TSOBC.

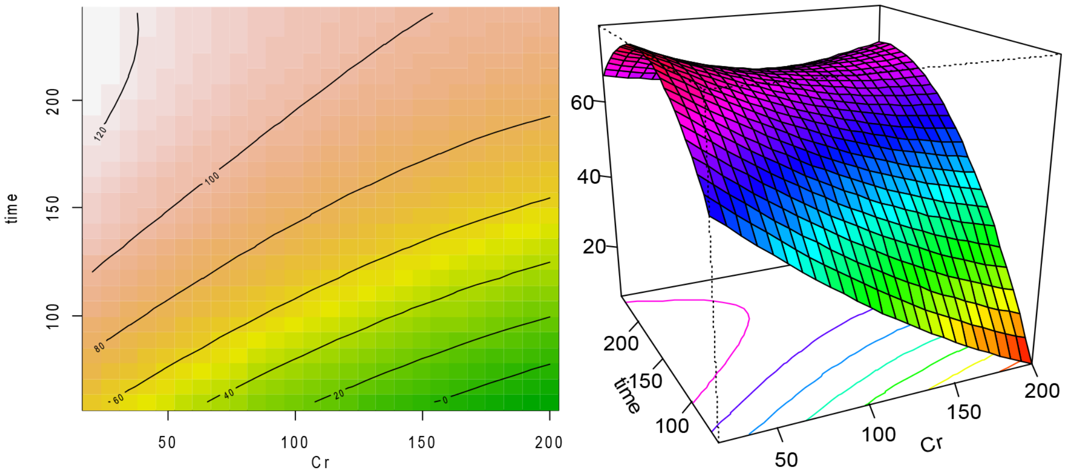

Fig. 11. Contour and 3D plots showing relation between Cr(VI) concentration and time for chromium removal.

in contact time until a specified value, the removal efficiency increases. This was due to the availability of a large number of vacant surface binding sites for adsorption of chromium during the initial stage, and after a lapse of time, the remaining unsaturated surface sites were difficult to occupy because of repulsive forces between the contaminant molecules in the aqueous environment and those on the adsorbent surface. At lower initial Cr(VI) concentration, chromium removal would increase as more active metal binding sites would be available for less number of contaminant ions.

3.4. Process optimization and confirmation

To obtain the optimum condition for Cr(VI) removal through the model equation predicted by RSM, the Solver "Add-ins" was applied using reasonable criteria. Optimized values of pH, TSOBC dose, initial Cr(VI) concentration and contact time were found as 3.7, 1.40 g/L, 77 mg/L and 180 min, respectively. To confirm the validity of the predicted results by the model, some additional experiments were conducted in three replicates. The results were in good agreement with those predicted by the Solver.

3.5. Adsorption isotherms

The application of adsorption process on the industrial scale requires proper determination of the sorption equilibrium for process simulation. The Langmuir and Freundlich equations have been frequently used to give the sorption equilibriums [54,57]. The Langmuir isotherm describes monolayer adsorption of contaminant onto adsorbent surface with a finite number of identical sites without any interaction between adsorbed ions. Inversely, Freundlich isotherm is an empirical equation for multilayer and heterogeneous adsorption sites [51]. Temkin model was based on how indirect adsorbent or adsorbate interactions influence the adsorption isotherms. Temkin model is the correction of Langmuir model, which introduces the influence of temperature on the adsorption process based on Langmuir model [41]. The Langmuir, Freundlich and Temkin equations are expressed as follows:

$$\text{Langmuir } Q_e = \frac{Q_{\max} K_L C_e}{1 + K_L C_e} \tag{6}$$

$$\text{Freundlich } Q_e = K_F C_e^{\frac{1}{n}} \tag{7}$$

$$\text{Temkin } Q_e = B \ln A + B \ln C_e \tag{8}$$

For Langmuir and Freundlich, Q_e (mg/g) is the equilibrium Cr(VI) ions concentration in the solid phase; $Q_{\max}$ (mg/g) is the maximum amount of sorption; K_L (L/mg) is the Langmuir sorption equilibrium constant; C_e is the concentration of solute at equilibrium or after adsorption; K_F (mg/g) (L/mmol)$^{1/n}$ is the Freundlich constant representing the sorption capacity and n is the constant depicting the sorption intensity [58].

For Temkin isotherm, $B = RT/b$, where A is the Temkin isotherm constant (L/g), R is the universal gas constant (8.314 J/mol K), b is the Temkin constant related to sorption heat (J/mol) and T is the temperature at 298 K [51].

The maximum adsorption capacity of TSOBC was obtained from the isotherm studies. Thus, batch adsorption isotherm tests were carried out at different initial concentrations from 20 to 200 mg/L under optimized conditions at pH around 3.7 and temperature of 25°C. The correlation coefficients (R^2) of these isotherms for Cr(VI) on each adsorbent and also the other relevant parameters are summarized in Table 5. The results showed the best fit to the Langmuir isotherm model for Cr(VI), indicating that the monolayer phase of Cr(VI) ions covers along TSOBC surface (Fig. 12). Accordingly, maximum adsorption capacity of TSOBC for Cr(VI) was 124.10 mg/g. Maximum adsorption capacity obtained in the present study was also compared with other related studies (Table 6).

3.6. Adsorption kinetics

The adsorption kinetic, an important physicochemical parameter, describes the rate of contaminant ions uptake on adsorbent and this rate controls the equilibrium time. The kinetics of contaminant removal is required for selecting optimum operating conditions for designing and modeling the adsorption processes. Different mechanisms such as film diffusion, pore diffusion or chemical reaction controls adsorption kinetics. The kinetic study was performed by placing 1.4 g of adsorbent in 1 L solution of initial concentration 200 mg/L at an optimum pH 3.7 under varying time interval (30–240 min) at 25°C and 150 rpm. In this study, the most popular kinetic models such as pseudo-first-order and pseudo-second-order were applied for analysis of adsorption data. Generally, the linear form of pseudo-first-model is expressed as follows [54,67–69]:

$$\log(q_e - q_t) = \log q_e - \frac{k_1}{2.303} \cdot t \tag{9}$$

where q_e and q_t are the amounts of Cr(VI) adsorbed at equilibrium and at time t (min), respectively, and k_1 is pseudo-first-order reaction constant (min^{-1}).

Table 5
Isotherm parameters for Cr(VI) adsorption on TSOBC

Isotherm	Parameters	Values
Langmuir	$Q_{\max}$ (mg/g)	124.1
	K_L (L/mg)	0.90
	R^2	0.99
	n	4.28
Freundlich	K_F (mg/g) (L/mmol)$^{1/n}$	62.32
	R^2	0.94
	A	0.39
Temkin	B	23.62
	R^2	0.98

Table 6
Comparison of maximum adsorption capacities of Cr(VI) by various adsorbents

Adsorbent	Adsorption capacity of Cr(VI) (mg/g)	References
Cross-linked chitosan/bentonite composite	89.13	[28]
Chitosan clay composite	142.31	[59]
Cross-linked chitosan–Fe(III) complex	148.40	[60]
Chitosan-cross-linked and non-cross-linked	78 and 50	[61]
Fuller's earth	23.58	[62]
Modified magnetic chitosan microspheres	233.1	[63]
Chitosan cross-linking with epichlorohydrin	11.3	[64]
Metal-ion imprinted chitosan	51	[65]
Chitosan/clay nanocomposite	357.13	[66]
TSOBC	124.1	This study

A straight line plot of log(q_e − q_t) vs. t will yield q_e and k_1 values from the intercept and slope, respectively. The constants of kinetic and correlation coefficients for pseudo-first-order plots are summarized in Table 7. A pseudo-second-order kinetic model is given as follows [70–72]:

$$\frac{t}{q_t} = \frac{1}{k_2 q_e^2} + \frac{1}{q_e} \cdot t \tag{10}$$

where k_2 is the pseudo-second-order rate constant (g/min). The results of the kinetic studies are shown in Fig. 13 and Table 7. The regression coefficients (R^2) demonstrated that the pseudo-second-order model fitted the experimental data better than pseudo-first-order model, with correlation coefficients of 0.99. This indicates that the sorption process of Cr(VI) onto TSOBC might be chemisorption. Chemisorption involves the formation of chemical bonds between the adsorbate and adsorbent. The suitability of the second-order kinetic model was also reported in the literature for the removal of chromium for the other adsorbents [73].

3.7. Thermodynamic study

In order to evaluate the thermodynamic behavior of adsorption of Cr(VI) by TSOBC, the adsorption experiments were carried out at different temperatures. The thermodynamic parameters, including enthalpy change (ΔH°), entropy change (ΔS°) and Gibbs free energy change (ΔG°), were investigated. The Gibbs free energy indicates the degree of spontaneity of the adsorption process, where more negative values reflect a more energetically favorable adsorption process. The Gibbs free energy (ΔG°) for the adsorption process was obtained using the following formula [74–77]:

$$\Delta G^\circ = -RT\ln K_L \tag{11}$$

$$\mathrm{Ln}K_L = \frac{\Delta S^\circ}{R} - \frac{\Delta H^\circ}{RT} \tag{12}$$

where ΔS° is the entropy change (J/mol K), ΔH° is the enthalpy change (J/mol), ΔG° is the Gibbs free energy change (J/mol), R is the ideal gas constant (8.314 J/K mol) and T is the absolute temperature (K) [78].

The ΔH° and ΔS° values given in Table 8 were calculated using the van't Hoff plot (Fig. 14), the plot of lnK_L vs. 1/T. Thermodynamic parameters are obtained at different temperatures of 298, 303, 308 and 313 K. As seen in Table 8, all values of ΔG° (–14.55, –11.19, –9.57 and –7.28 kJ/mol) were negative for all the studied temperatures indicating the adsorption of Cr(VI) on TSOBC was feasible and spontaneous. Actually that the values of the ΔG° decrease with increasing

Table 7
Constants obtained from kinetic models for Cr(VI) adsorption onto TSOBC

C_0 (mg/L)	Pseudo-first-order			Pseudo-second-order		
	q_e (mg/g)	k_1 (min^{-1})	R^2	q_e (mg/g)	k_2 (min^{-1})	R^2
200	116.49	0.002	0.92	120	0.002	0.99

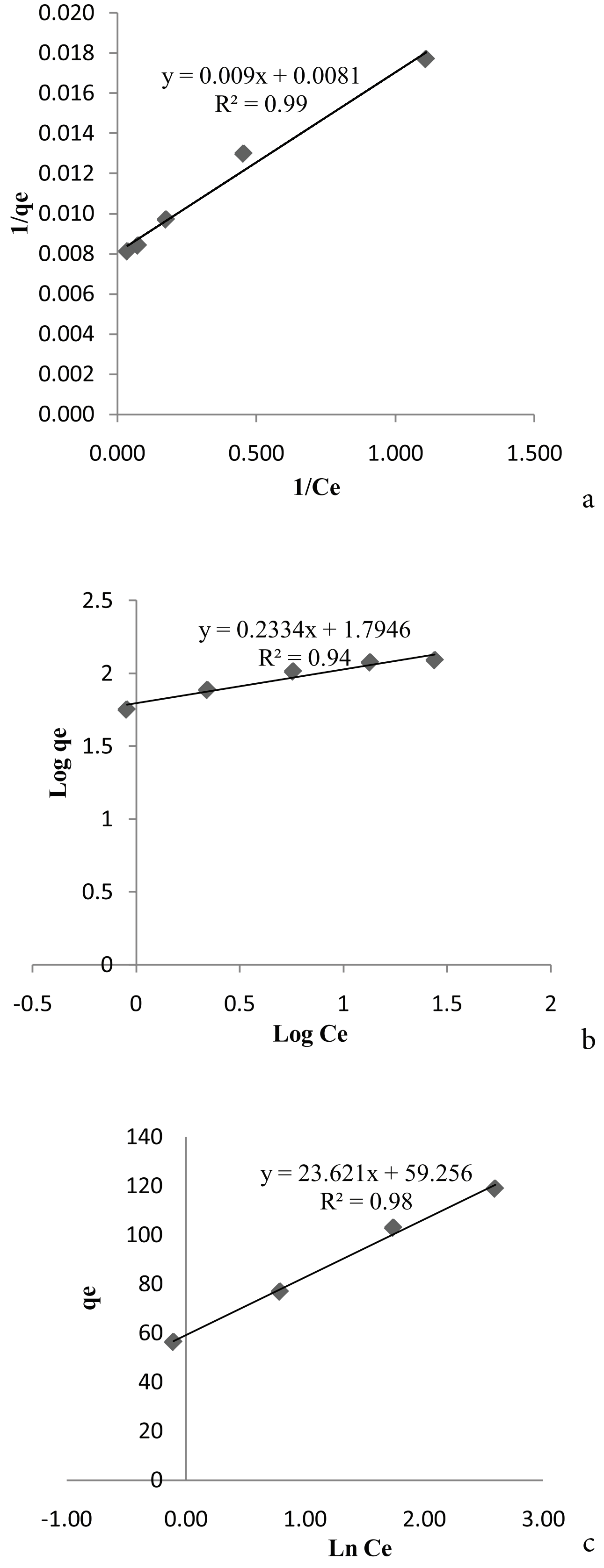

Fig. 12. Langmuir (a), Freundlich (b) and Temkin (c) plots for the adsorption of Cr(VI) by TSOBC.

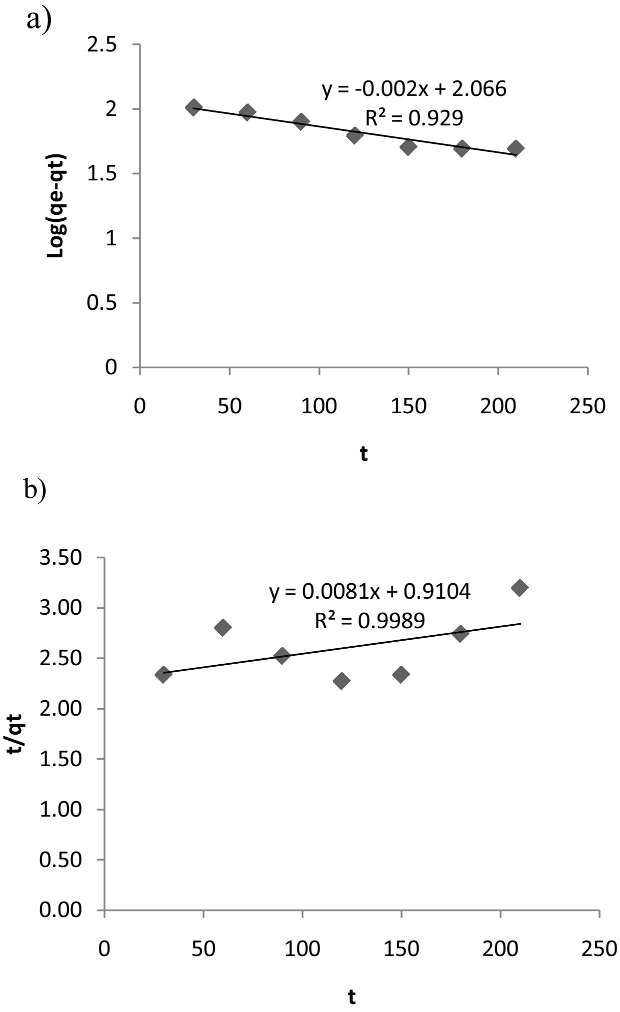

Fig. 13. Pseudo-first-order (a) and pseudo-second-order model (b) for adsorption of Cr(VI) by TSOBC.

temperature indicating the increase of spontaneous influence. The negative value of $\Delta S°$ (−48.99 J/mol K) belongs to a decline in the degrees of freedom of the adsorbed chromium species [11]. However, a considerable change of entropy can be observed showing that TSOBC change significantly as a result of adsorption. Furthermore, the positive value of $\Delta H°$ (165.44 kJ/mol) also confirms the endothermic nature of the adsorption of Cr(VI) on TSOBC and increasing temperature favors the adsorption process [79,80].

4. Conclusions

The results of the present work suggest that TSOBC is an excellent adsorbent for effective removal of Cr(VI) from aqueous environment. In this study, the experimental design of runs and the statistical analysis of the data were done using RSM in "R" software. The results suggest that the selected quadratic model was adequate in predicting the response variables for the experimental data. The obtained experimental results were found to be in good agreement with predicted values by the model. The model quality was tested

Table 8
Thermodynamic parameters for adsorption of Cr(VI) onto TSOBC

Adsorbent	Temperature (K)	$\Delta G°$ (kJ/mol)	$\Delta H°$ (kJ/mol)	$\Delta S°$ (kJ/mol K)	R^2
TSOBC	298	–14.55	165.44	–48.99	0.98
	303	–11.19			
	308	–9.57			
	313	–7.28			

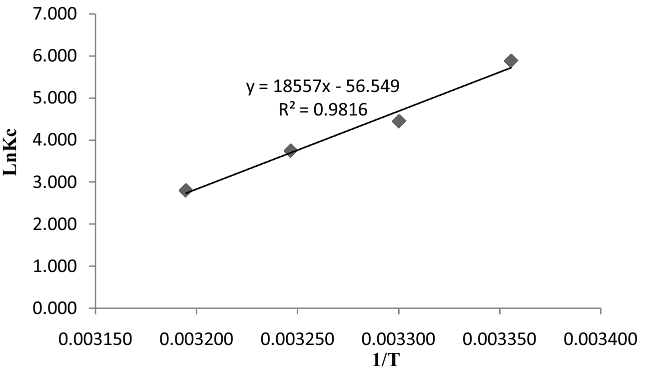

Fig. 14. Van't Hoff plot for thermodynamic parameters.

through LOF, *F* and *P* values. Optimized values of pH, adsorbent dosage, initial Cr(VI) concentration and contact time were found as 3.7, 1.4 g/L, 77 mg/L and 180 min, respectively. The TSOBC was characterized by SEM, XRD, EDX and FTIR techniques. The SEM micrograph of TSOBC before adsorption revealed fractured and rough surface morphology providing better adsorption sites. The adsorption capacity of Cr(VI) onto natural bentonite was very low. After modification using chitosan and cationic surfactant, its removal percentage enhanced significantly. Results from the analysis of response surfaces indicated that pH, the adsorbent dosage, Cr(VI) concentration and time were found to have significant effects on the adsorption efficiency of Cr(VI). In this study, we used chitosan with a degree of deacetylation of 90% for our work. Because, chitosan with a degree of deacetylation more than 90% has not given further significant increase in adsorption efficiency. In addition, from the economic consideration, chitosan with a degree of deacetylation 90% is the best choice for Cr(VI) removal, as it has good solubility and it is not too expensive. The adsorption isotherms and kinetics were also investigated. Among the isotherm models tested, Langmuir isotherm model was found to be the best fit for the obtained data, with the maximum adsorption capacity of 124.10 mg/g, thus indicating a monolayer adsorption behavior. The adsorption kinetics indicated that hexavalent chromium adsorption on TSOBC followed pseudo-second-order better than pseudo-first-order model. Moreover, thermodynamic studies showed that adsorption of Cr(VI) on TSOBC was feasible, spontaneous and endothermic in nature.

Acknowledgments

The authors wish to gratefully thank Dr. Mehdi Zarrei for his useful advice for improving the paper. We also wish to thank Mansoureh Farhang, Mehdi Ghasemi, Mahmood Shams and Zohreh Moeini for their laboratory analysis, technical assistance and management support in Gonabad University of Medical Sciences. This research has been financially supported by the Tehran University of Medical Sciences, Institute for Environmental Research, branch of water research, code: 94-03-46-29993.

References

[1] C.d.G. Sampaio, L.S. Frota, H.S. Magalhães, L.M. Dutra, D.C. Queiroz, R.S. Araújo, M.T.S. Trevisan, Chitosan/mangiferin particles for Cr(VI) reduction and removal, Int. J. Biol. Macromol., 78 (2015) 273–279.

[2] M.H. Dehghani, G.-R. Jahed, A. Zarei, Investigation of low-pressure ultraviolet radiation on inactivation of Rhabitidae Nematode from water, Iran. J. Public Health, 42 (2013) 314.

[3] M. Fazlzadeh, R. Khosravi, A. Zarei, Green synthesis of zinc oxide nanoparticles using *Peganum harmala* seed extract, and loaded on *Peganum harmala* seed powdered activated carbon as new adsorbent for removal of Cr(VI) from aqueous solution, Ecol. Eng., 103 (2017) 180–190.

[4] Z. Hu, L. Lei, Y. Li, Y. Ni, Chromium adsorption on high-performance activated carbons from aqueous solution, Sep. Purif. Technol., 31 (2003) 13–18.

[5] R. Huang, B. Yang, Q. Liu, Y. Liu, Simultaneous adsorption of aniline and Cr(VI) ion by activated carbon/chitosan composite, J. Appl. Polym. Sci., 131 (2014).

[6] A. Kara, Adsorption of Cr(VI) ions onto poly (ethylene glycol dimethacrylate-1-vinyl-1,2,4-triazole), J. Appl. Polym. Sci., 114 (2009) 948–955.

[7] K. Selvaraj, S. Manonmani, S. Pattabhi, Removal of hexavalent chromium using distillery sludge, Bioresour. Technol., 89 (2003) 207–211.

[8] M. Pang, N. Kano, H. Imaizumi, Adsorption of chromium (VI) from aqueous solution using zeolite/chitosan hybrid composite, J. Chem. Chem. Eng., 9 (2015) 433–441.

[9] Y. Zhang, Y. Li, J. Li, G. Sheng, Y. Zhang, X. Zheng, Enhanced Cr(VI) removal by using the mixture of pillared bentonite and zero-valent iron, Chem. Eng. J., 185–186 (2012) 243–249.

[10] M. Fazlzadeh, K. Rahmani, A. Zarei, H. Abdoallahzadeh, F. Nasiri, R. Khosravi, A novel green synthesis of zero valent iron nanoparticles (NZVI) using three plant extracts and their efficient application for removal of Cr(VI) from aqueous solutions, Adv. Powder Technol., 28 (2017) 122–130.

[11] A. Naghizadeh, H. Shahabi, F. Ghasemi, A. Zarei, Synthesis of walnut shell modified with titanium dioxide and zinc oxide nanoparticles for efficient removal of humic acid from aqueous solutions, J. Water Health, 14 (2016) 989–997.

[12] A. Naghizadeh, Regeneration of carbon nanotubes exhausted with humic acid using electro-Fenton technology, Arabian J. Sci. Eng., 41 (2016) 155–161.

[13] A. El Nemr, Potential of pomegranate husk carbon for Cr(VI) removal from wastewater: kinetic and isotherm studies, J. Hazard. Mater., 161 (2009) 132–141.

[14] M. Ledin, K. Pedersen, B. Allard, Effects of pH and ionic strength on the adsorption of Cs, Sr, Eu, Zn, Cd and Hg by *Pseudomonas putida*, Water Air Soil Pollut., 93 (1997) 367–381.

[15] H. Golestanifar, B. Haibati, H. Amini, M.H. Dehghani, A. Asadi, Removal of hexavalent chromium from aqueous solution by adsorption on γ-alumina nanoparticles, Environ. Prot. Eng., 41 (2015) 133–145.

[16] M.H. Dehghani, A. Naghizadeh, A. Rashidi, E. Derakhshani, Adsorption of reactive blue 29 dye from aqueous solution by multiwall carbon nanotubes, Desal. Wat. Treat., 51 (2013) 7655–7662.

[17] M.H. Dehghani, A.H. Mahvi, N. Rastkari, R. Saeedi, S. Nazmara, E. Iravani, Adsorption of bisphenol A (BPA) from aqueous solutions by carbon nanotubes: kinetic and equilibrium studies, Desal. Wat. Treat., 54 (2015) 84–92.

[18] M. Dehghani, P. Mahdavi, I. Tyagi, S. Agarwal, V. Kumar Gupta, Investigating the toxicity of acid dyes from textile effluent under UV/ZnO process using *Daphnia magna*, Desal. Wat. Treat., 57 (2016) 24359–24367.

[19] M.H. Dehghania, B. Karimia, A. Rafieepourd, Continuous removal of toxic nickel from industrial wastewater by flotation-adsorption with multi-walled carbon nanotubes: kinetic and adsorption isotherms, Desal. Wat. Treat., 71 (2017) 107–115.

[20] M.H. Dehghani, M. Mostofi, M. Alimohammadi, G. McKay, K. Yetilmezsoy, A.B. Albadarin, J. Sahu, High-performance removal of toxic phenol by single-walled and multi-walled carbon nanotubes: kinetics, adsorption, mechanism and optimization studies, J. Ind. Eng. Chem., 35 (2016) 63–74.

[21] M.H. Dehghani, M. Faraji, A. Mohammadi, H. Kamani, Optimization of fluoride adsorption onto natural and modified pumice using response surface methodology: isotherm, kinetic and thermodynamic studies, Korean J. Chem. Eng., 34 (2017) 454–462.

[22] M. Shams, R. Nodehi, M. Alimohammadi, A. Mahvi, A survey of nitrate and fluoride in water distribution networks of Tabas, Iran, World Appl. Sci. J., 7 (2009) 1516–1520.

[23] C. Gerente, Y. Andres, G. Mckay, P. Le Cloirec, Removal of arsenic(V) onto chitosan: from sorption mechanism explanation to dynamic water treatment process, Chem. Eng. J., 158 (2010) 593–598.

[24] C. Septhum, S. Rattanaphani, J. Bremner, V. Rattanaphani, An adsorption study of Al(III) ions onto chitosan, J. Hazard. Mater., 148 (2007) 185–191.

[25] M. Arvand, M.A. Pakseresht, Cadmium adsorption on modified chitosan-coated bentonite: batch experimental studies, J. Chem. Technol. Biotechnol., 88 (2013) 572–578.

[26] W.W. Ngah, S. Fatinathan, N. Yosop, Isotherm and kinetic studies on the adsorption of humic acid onto chitosan-H_2SO_4 beads, Desalination, 272 (2011) 293–300.

[27] S. Ramnani, S. Sabharwal, Adsorption behavior of Cr(VI) onto radiation crosslinked chitosan and its possible application for the treatment of wastewater containing Cr(VI), React. Funct. Polym., 66 (2006) 902–909.

[28] Q. Liu, B. Yang, L. Zhang, R. Huang, Adsorptive removal of Cr(VI) from aqueous solutions by cross-linked chitosan/bentonite composite, Korean J. Chem. Eng., 32 (2015) 1314–1322.

[29] S. Hasan, A. Krishnaiah, T.K. Ghosh, D.S. Viswanath, V.M. Boddu, E.D. Smith, Adsorption of divalent cadmium (Cd(II)) from aqueous solutions onto chitosan-coated perlite beads, Ind. Eng. Chem. Res., 45 (2006) 5066–5077.

[30] W.S.W. Ngah, N.F.M. Ariff, M.A.K.M. Hanafiah, Preparation, characterization, and environmental application of crosslinked chitosan-coated bentonite for tartrazine adsorption from aqueous solutions, Water Air Soil Pollut., 206 (2010) 225–236.

[31] L. Wang, A. Wang, Adsorption characteristics of Congo Red onto the chitosan/montmorillonite nanocomposite, J. Hazard. Mater., 147 (2007) 979–985.

[32] K.I. Benabadji, A. Mansri, Chromium removal using poly(4-vinylpyridinium)-modified treated clay salts, Desal. Wat. Treat., 52 (2014) 5931–5941.

[33] C.-B. Esma, D. Zoulikha, B. Kamel Ismet, M. Ali, Molecular weight effect on chromium(VI) retention by poly(N-octyl-4-vinylpyridinium bromide) copolymers, Desal. Wat. Treat., 52 (2014) 6474–6480.

[34] V.M. Boddu, K. Abburi, J.L. Talbott, E.D. Smith, Removal of hexavalent chromium from wastewater using a new composite chitosan biosorbent, Environ. Sci. Technol., 37 (2003) 4449–4456.

[35] Y. Vijaya, S.R. Popuri, V.M. Boddu, A. Krishnaiah, Modified chitosan and calcium alginate biopolymer sorbents for removal of nickel (II) through adsorption, Carbohydr. Polym., 72 (2008) 261–271.

[36] R. Huang, D. Zheng, B. Yang, B. Wang, Preparation and simultaneous sorption of CTMAB-HTCC bentonite towards aniline and Cr (VI), Energy Sources Part A, 38 (2016) 519–526.

[37] Y. Xi, R.L. Frost, H. He, T. Kloprogge, T. Bostrom, Modification of Wyoming montmorillonite surfaces using a cationic surfactant, Langmuir, 21 (2005) 8675–8680.

[38] R. Naidu, N. Sethunathan, Sorption-Desorption of Fenamiphos in Surfactant-Modified Clays, N. Singh, M. Megharaj, W.P. Gates, J. Churchman, R.S. Kookana, Eds., Bulletin of Environmental Contamination and Toxicology, Vol. 72, 2004, pp. 276–282.

[39] V.A. Oyanedel-Craver, J.A. Smith, Effect of quaternary ammonium cation loading and pH on heavy metal sorption to Ca bentonite and two organobentonites, J. Hazard. Mater., 137 (2006) 1102–1114.

[40] A.A. Atia, Adsorption of chromate and molybdate by cetylpyridinium bentonite, Appl. Clay Sci., 41 (2008) 73–84.

[41] J. Guo, S. Chen, L. Liu, B. Li, P. Yang, L. Zhang, Y. Feng, Adsorption of dye from wastewater using chitosan–CTAB modified bentonites, J. Colloid Interface Sci., 382 (2012) 61–66.

[42] R. Huang, D. Zheng, B. Yang, B. Wang, Z. Zhang, Preparation and characterization of CTAB-HACC bentonite and its ability to adsorb phenol from aqueous solution, Water Sci. Technol., 64 (2011) 286–292.

[43] K. Ba, L. He, H. Tang, J. Gao, S. Zhu, Y. Li, W. Sun, Use of chitosan-modified bentonite for removal of Cu^{2+}, Cl^- and 2,4-dichlorophenoxyacetic acid (2,4-D) from aqueous solution, J. Chem. Chem. Eng., 63 (2014) 253–258.

[44] R.V. Lenth, Response-surface methods in R using RSM, J. Stat. Software, 32 (2009) 1–17.

[45] S. Kalyani, A. Krishnaiah, V.M. Boddu, Adsorption of divalent cobalt from aqueous solution onto chitosan–coated perlite beads as biosorbent, Sep. Sci. Technol., 42 (2007) 2767–2786.

[46] Y. Liu, Y. Zheng, A. Wang, Response surface methodology for optimizing adsorption process parameters for methylene blue removal by a hydrogel composite, Adsorpt. Sci. Technol., 28 (2010) 913–922.

[47] J. Qu, G. Liu, Y. Wang, R. Hong, Preparation of Fe_3O_4–chitosan nanoparticles used for hyperthermia, Adv. Powder Technol., 21 (2010) 461–467.

[48] D.W.G. Wang, W. Li, K. Chen, Preparation and absorbability for Orange II of CTAB modified bentonite, Adv. Mater. Res., 807–809 (2013) 530–533.

[49] M. Amini, H. Younesi, N. Bahramifar, A.A.Z. Lorestani, F. Ghorbani, A. Daneshi, M. Sharifzadeh, Application of response surface methodology for optimization of lead biosorption in an aqueous solution by *Aspergillus niger*, J. Hazard. Mater., 154 (2008) 694–702.

[50] M. Shams, M.H. Dehghani, R. Nabizadeh, A. Mesdaghinia, M. Alimohammadi, A.A. Najafpoor, Adsorption of phosphorus from aqueous solution by cubic zeolitic imidazolate framework-8: modeling, mechanical agitation versus sonication, J. Mol. Liq., 224 (2016) 151–157.

[51] M.R. Samarghandi, M. Zarrabi, A. Amrane, M.N. Sepehr, M. Noroozi, S. Namdari, A. Zarei, Kinetic of degradation of two azo dyes from aqueous solutions by zero iron powder: determination of the optimal conditions, Desal. Wat. Treat., 40 (2012) 137–143.

[52] W.W. Ngah, A. Kamari, S. Fatinathan, P. Ng, Adsorption of chromium from aqueous solution using chitosan beads, Adsorption, 12 (2006) 249–257.

[53] D.-W. Cho, B.-H. Jeon, C.-M. Chon, Y. Kim, F.W. Schwartz, E.-S. Lee, H. Song, A novel chitosan/clay/magnetite composite for adsorption of Cu(II) and As(V), Chem. Eng. J., 200 (2012) 654–662.

[54] R. Khosravi, M. Fazlzadehdavil, B. Barikbin, A.A. Taghizadeh, Removal of hexavalent chromium from aqueous solution by granular and powdered Peganum Harmala, Appl. Surf. Sci., 292 (2014) 670–677.

[55] M. Rao, A. Parwate, A. Bhole, Uptake of nickel from aqueous solution by adsorption using low cost adsorbents, Pollut. Res., 20 (2001) 669–675.

[56] A. Shanmugapriya, R. Ramya, S. Ramasubramaniam, P. Sudha, Studies on removal of Cr(VI) and Cu(II) ions using chitosan grafted-polyacrylonitrile, Arch. Appl. Sci. Res., 3 (2011) 424–435.

[57] A. Kara, N. Tekin, A. Alan, A. Şafaklı, Physicochemical parameters of Hg(II) ions adsorption from aqueous solution by sepiolite/poly (vinylimidazole), J. Environ. Chem. Eng., 4 (2016) 1642–1652.

[58] R. Ansari, B. Seyghali, A. Mohammad-Khah, M.A. Zanjanchi, Highly efficient adsorption of anionic dyes from aqueous solutions using sawdust modified by cationic surfactant of cetyltrimethylammonium bromide, J. Surfactants Deterg., 15 (2012) 557–565.

[59] M. Auta, B. Hameed, Chitosan–clay composite as highly effective and low-cost adsorbent for batch and fixed-bed adsorption of methylene blue, Chem. Eng. J., 237 (2014) 352–361.

[60] C.A. Demarchi, A. Debrassi, J. Dal Magro, N. Nedelko, A. Ślawska-Waniewska, P. Dłużewski, C.A. Rodrigues, Adsorption of Cr(VI) on crosslinked chitosan–Fe(III) complex in fixed-bed systems, J. Water Process Eng., 7 (2015) 141–152.

[61] V.K. Singh, P.N. Tiwari, Removal and recovery of chromium(VI) from industrial waste water, J. Chem. Technol. Biotechnol., 69 (1997) 376–382.

[62] A. Bhattacharya, T. Naiya, S. Mandal, S. Das, Adsorption, kinetics and equilibrium studies on removal of Cr(VI) from aqueous solutions using different low-cost adsorbents, Chem. Eng. J., 137 (2008) 529–541.

[63] X. Sun, Q. Li, L. Yang, H. Liu, Chemically modified magnetic chitosan microspheres for Cr(VI) removal from acidic aqueous solution, Particuology, 26 (2016) 79–86.

[64] B. Hastuti, A. Masykur, S. Hadi, Modification of Chitosan by Swelling and Crosslinking Using Epichlorohydrin as Heavy Metal Cr(VI) Adsorbent in Batik Industry Wastes, IOP Conference Series: Materials Science and Engineering, IOP Publishing, 2016.

[65] T. Tianwei, H. Xiaojing, D. Weixia, Adsorption behaviour of metal ions on imprinted chitosan resin, J. Chem. Technol. Biotechnol., 76 (2001) 191–195.

[66] S. Pandey, S.B. Mishra, Organic–inorganic hybrid of chitosan/organoclay bionanocomposites for hexavalent chromium uptake, J. Colloid Interface Sci., 361 (2011) 509–520.

[67] M. Hassanzadeh, M. Kambarani, L. Tayebi, F. Yazdian, Kinetic study of sodium cocoyl sarcosinate synthesis and factors affecting the reaction on bench and pilot scales, J. Surfactants Deterg., 15 (2012) 551–556.

[68] Y. Ho, G. McKay, A comparison of chemisorption kinetic models applied to pollutant removal on various sorbents, Process Saf. Environ. Prot., 76 (1998) 332–340.

[69] A. Kara, E. Demirbel, N. Tekin, B. Osman, N. Beşirli, Magnetic vinylphenyl boronic acid microparticles for Cr(VI) adsorption: kinetic, isotherm and thermodynamic studies, J. Hazard. Mater., 286 (2015) 612–623.

[70] R. Pandimurugan, S. Thambidurai, Novel seaweed capped ZnO nanoparticles for effective dye photodegradation and antibacterial activity, Adv. Powder Technol., 27 (2016) 1062–1072.

[71] N. Kataria, V. Garg, M. Jain, K. Kadirvelu, Preparation, characterization and potential use of flower shaped Zinc oxide nanoparticles (ZON) for the adsorption of Victoria Blue B dye from aqueous solution, Adv. Powder Technol., 27 (2016) 1180–1188.

[72] F. Fadzil, S. Ibrahim, M.A.K.M. Hanafiah, Adsorption of lead(II) onto organic acid modified rubber leaf powder: batch and column studies, Process Saf. Environ. Prot., 100 (2016) 1–8.

[73] A.C. Zimmermann, A. Mecabô, T. Fagundes, C.A. Rodrigues, Adsorption of Cr(VI) using Fe-crosslinked chitosan complex (Ch-Fe), J. Hazard. Mater., 179 (2010) 192–196.

[74] H. Abdoallahzadeh, B. Alizadeh, R. Khosravi, M. Fazlzadeh, Efficiency of EDTA modified nanoclay in removal of humic acid from aquatic solutions, J. Mazandaran Univ. Med. Sci., 26 (2016) 111–125.

[75] M. Pirsaheb, A. Dargahi, S. Hazrati, M. Fazlzadehdavil, Removal of diazinon and 2,4-dichlorophenoxyacetic acid (2,4-D) from aqueous solutions by granular-activated carbon, Desal. Wat. Treat., 52 (2014) 4350–4355.

[76] F.M. Sannaningannavar, S.N. Patil, R.M. Melavanki, B.S. Navati, N.H. Ayachit, Thermodynamic parameters and their dependence on temperature in the range 298–353 K for ethoxylated sorbitan ester tween 20, 40, 60 and 80 surfactants, J. Surfactants Deterg., 18 (2015) 495–504.

[77] M. Entezai, A. Fazlzadeh, A. Ahmadfazeli, R. Khosravi, Removal of cephalexin using green montmorillonite loaded with TiO_2 nanoparticles in the presence potassium permanganate from aqueous solution, Environ. Health Suppl., 18 (2014) 388–396.

[78] M.H. Dehghani, A. Zarei, A. Mesdaghinia, R. Nabizadeh, M. Alimohammadi, M. Afsharnia, Response surface modeling, isotherm, thermodynamic and optimization study of arsenic (V) removal from aqueous solutions using modified bentonite-chitosan (MBC), Korean J. Chem. Eng., 34 (2015) 1–11.

[79] K. Hernández-Hernández, M. Solache-Ríos, M. Díaz-Nava, Removal of brilliant blue FCF from aqueous solutions using an unmodified and iron-modified bentonite and the thermodynamic parameters of the process, Water Air Soil Pollut., 224 (2013) 1562.

[80] E. Derakhshani, A. Naghizadeh, A.R. Yari, M.J. Mohammadi, M. Kamranifar, M. Farhang, Association of toxicochemical and microbiological quality of bottled mineral water in Birjand city, Iran, Toxin Rev., (2017) 1–6.